9th AUSTRALASIAN
FLUID MECHANICS CONFERENCE,
AUCKLAND, 8-12 DECEMBER 1986

Numerical Simulation of Turbulent Flow in a Concentric Annulus

P. G. HOLLAND[1] and C. A. J. FLETCHER[2]

[1]CSIRO Division of Energy Chemistry, Lucas Heights.
[2]Department of Mechanical Engineering, University of Sydney, Australia.

ABSTRACT

A parabolised method of solving the Navier-Stokes equations is developed, which does not have the characteristic limit on the minimum axial step size. A simple turbulence model is chosen which uses the concepts of eddy viscosity and mixing length. The reduced set of equations is capable of predicting developing and fully developed flow in a concentric annulus. Wall shear stresses and Reynolds stress profiles compare well with experimental data.

INTRODUCTION

Annular geometries are used in many important engineering structures. One example is the nuclear reactor fuel assembly. Annular test sections are often used to evaluate the heat transfer performance of various types of fuel element. Annular flow is also found in some propulsion systems and in fluid flow equipment used by the thermal process industry.

Annular flow is additionally interesting because it might provide insight into the general problem of fully developed turbulent shear flows. Fully developed annular flow involves the combination of two boundary layers (each extending from a wall to, perhaps, a position of maximum velocity) which, unlike those that meet at the centre of a pipe or midway between parallel planes, may have quite different velocity distribution, shear stress and turbulence characteristics.

In addition, the two one-dimensional, fully developed turbulent flows which have been studied in detail - flow in circular pipes and between parallel planes - are both limiting cases of annular pipe flow.

Most numerical studies of annular flow use iterative methods, because they are based on a non-parabolic system of differential equations ; in this investigation, however, the axial diffusion term is deleted as well as other terms which are negligibly small, so that the Navier-Stokes equations may be solved in a reduced form. This method of reducing equations is only valid when there is a dominant flow direction and when the flow has minimal upstream influence.

Fluctuations in turbulence are represented by Reynolds stress terms which are modelled using mixing length expressions. The Reynolds stress terms may be reduced, as are the other terms in the Navier-Stokes equations, so that the non-elliptic nature of the algorithm is preserved.

In the present paper, the set of governing equations is presented and it is shown how they may be reduced by discarding insignifiant terms. Details of the numerical grid are given, and a simple turbulence model is described. The method of solving the reduced equations follows and the results demonstrate how the algorithm compares with experimental data.

GOVERNING EQUATIONS

The steady-state momentum equations given (Bird, Stewart and Lightfoot, 1960) in cylindrical coordinates (x, r) may be expanded and expressed non-dimensionally in the absence of swirl as

$$v\frac{\partial u}{\partial r} + u\frac{\partial u}{\partial r} = -\frac{\partial P}{\partial x} + \frac{1}{Re}\left[\frac{\partial^2 u}{\partial r^2} + \frac{1}{r}\cdot\frac{\partial u}{\partial r} + \frac{\partial^2 u}{\partial x^2}\right] \quad ..(1)$$

$$v\frac{\partial v}{\partial r} + u\frac{\partial v}{\partial r} = -\frac{\partial P}{\partial r} + \frac{1}{Re}\left[\frac{1}{r}\cdot\frac{\partial v}{\partial r} - \frac{v}{r^2} + \frac{\partial^2 v}{\partial r^2} + \frac{\partial^2 v}{\partial x^2}\right] \quad ..(2)$$

where u and v represent the velocity coordinates in the axial and radial directions, P represents pressure and Re represents Reynolds number defined as $D_h U_m/\nu$, where D_h, hydraulic diameter, is defined as 2 $(R_o - R_i)$, R_o and R_i being the outer and inner radii of the annulus, U_m represents the maximum axial velocity and ν is the kinematic viscosity.

The steady-state equation of continuity is expressed in cylindrical cordinates for axisymmetric, incompressible flow as

$$\frac{\partial (rv)}{\partial r} + r\frac{\partial u}{\partial x} = 0 \quad \ldots (3)$$

If equations (1), (2) and (3) are solved iteratively on a digital computer, provision must be made to store all variables at each nodal point, many sweeps being made over the domain. Large amounts of computer time and storage are required before convergence is achieved. In the following section it is shown how these equations may be simplified so that they may be solved numerically with a single sweep at successive downstream stations across the domain.

Reduction of the Governing Equation

For flows which have a dominant axial flow direction and an insignificant upstream influence, the Navier-Stokes equations may be simplified ; in practice this applies everywhere except near the entrance region (Holland and Fletcher, 1985). The conditions which provide such a simplification may be stated (Schlichting, 1955).

$$\text{(a)}\quad u \approx 1, \quad \text{(b)}\quad L \gg Y, \quad \text{(c)}\quad \delta < Y/2 \quad \ldots(4)$$

Y being equal to the radial gap, $R_o - R_i$.
Stated explicitly, these conditions indicate that

(a) the equations are non-dimensionalised such that the axial velocity assumes a value close to unity.
(b) the entry length (L) of the annulus far exceeds the radial gap Y, which is valid except near the entrance region, and
(c) the boundary layer thickness (δ) cannot exceed half of the radial gap, because there is a boundary layer adjacent to each radial boundary.

Making an estimate of the order-of-magnitude of each term we obtain

$$\frac{\partial u}{\partial x} \approx \frac{1}{L}, \frac{\partial^2 u}{\partial x^2} \approx \frac{1}{L^2}, \frac{\partial u}{\partial r} \approx \frac{1}{\delta}, \frac{\partial^2 u}{\partial r^2} \approx \frac{1}{\delta^2},$$

$$\frac{\partial v}{\partial x} \approx \frac{Y}{L^2}, \frac{\partial^2 v}{\partial x^2} \approx \frac{Y}{L^3}, \frac{\partial v}{\partial r} \approx \frac{1}{L}, \frac{\partial^2 v}{\partial r^2} \approx \frac{1}{Y.L}, \quad \ldots(5)$$

By substituting equation (5) into equations (1) and (2) we can neglect the two second-derivative terms w.r.t. x (Yaschin et al. 1984), thus producing the following equations:

$$v\frac{\partial u}{\partial r} + u\frac{\partial u}{\partial x} = -\frac{\partial P}{\partial x} + \frac{1}{Re}\left[\frac{\partial^2 u}{\partial r^2} + \frac{1}{r}.\frac{\partial u}{\partial r}\right] \quad \ldots(6)$$

$$v\frac{\partial v}{\partial r} + u\frac{\partial v}{\partial x} = -\frac{\partial P}{\partial r} + \frac{1}{Re}\left[\frac{1}{r}.\frac{\partial v}{\partial r} - \frac{v}{r^2} + \frac{\partial^2 v}{\partial r^2}\right] \ldots(7)$$

Equations (6), (7) and the continuity equation (3) constitute a non-parabolic set : the term $u.\partial v/\partial x$ in (7) introduces a strongly elliptic character into the equations (Armfield and Fletcher, 1986). To remove this influence, the radial momentum equation (7) is again reduced. Let the pressure be split as follows:

$$P = P_1 + P_2 \quad \ldots(8)$$

where P_1 = P(x) , the pressure component in the axial direction, and
P_2 = P(r) , the pressure component in the radial direction in non-swirling flow.

From equation (7),

$$\frac{\partial P}{\partial r} = -v\frac{\partial v}{\partial r} - u\frac{\partial v}{\partial x} + \frac{1}{Re}\left[\frac{1}{r}.\frac{\partial v}{\partial r} - \frac{v}{r^2} + \frac{\partial^2 v}{\partial r^2}\right] \quad \ldots(9)$$

An order-of-magnitude estimate yields $P_2 \approx Y/L^2$. From equation (6) $P \approx 1$ and since $Y/L^2 \ll 1$, P may now be defined as $P = P_1$, rather than the definition given by equation (8).

Equation (7) is then reduced to $\frac{\partial P}{\partial r} = 0 \quad \ldots(10)$

Equations (3), (6) and (10) now provide the set of parabolised governing equations, which will be solved numerically, together with the appropriate boundary conditions, i.e.

$$\left.\begin{aligned} u\,(R_i, x) = v\,(R_i, x) = 0 \\ u\,(R_o, x) = v\,(R_o, x) = 0 \end{aligned}\right\} \quad \ldots(11)$$

for $0 \leq x \leq X$, where X is the total axial length

DISCRETISATION SCHEME

A rectangular grid with variable radial and axial mesh length is used. To resolve the flow adequately in the viscous sublayer adjacent to either radial boundary, it is necessary to place several nodes near the boundary wall. Adjacent nodes are placed so that the radial spacing increases gradually from the wall until the radial limit or the mean radius is reached. For convenience, the radial nodes are symmetrically disposed about the mean radius of the annulus. Figure 1 illustrates the computational grid used.

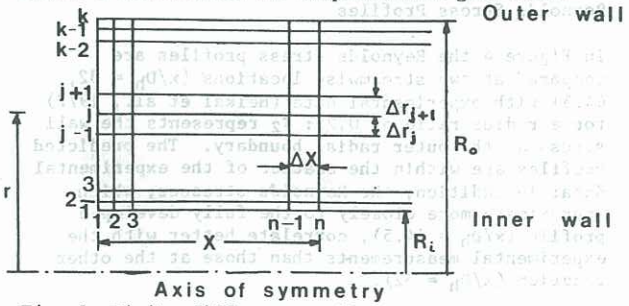

Fig 1. Finite-difference grid

The initial limits set for the grid aspect ratio ($\Delta x/\Delta r$), were 2 near the radial wall and 0.5 near the mean radius : at higher Reynolds numbers, however, these limits can be stretched to between 10 and 0.1 without any significant change in accuracy, thus achieving substantial savings in computing time.

In Figure 2, $\Delta x = 0.002$ and Δr varied between 0.001 and 0.0046, giving 201 radial nodes ; in Figure 3, on the other hand, $\Delta x = 0.005$ and there were approximately 70 radial nodes in each of the two cases.

Radial derivatives are discretised as follows; the first derivative, $\partial f/\partial r$ becomes

$$\left[\frac{f_{j+1} - f_{j-1}}{\Delta r_{j+1} + \Delta r_j}\right] + O(\Delta r^2),$$

and the second derivative $\partial^2 f/\partial r^2$ becomes

$$\left[\left(\frac{f_{j+1} - f_j}{\Delta r_{j+1}}\right) - \left(\frac{f_j - f_{j-1}}{\Delta r_j}\right)\right] \Bigg/ \left(\frac{\Delta r_{j+1} + \Delta r_j}{2}\right) + O(\Delta^2 r),$$

where $\Delta r_{j+1} = r_{j+1} - r_j$.

TURBULENCE

To include the turbulence contribution, the governing equations are expressed in terms of mean flow and non-stationary quantities before averaging. The only extra term arising from the absence of swirl is the Reynolds stress, $\overline{u'v'}$, which is added to the axial momentum equation : the algebraic eddy viscosity approach allows the shear stress to be related to the mean velocity component as follows:

$$\overline{u'v'} = \nu_x.\partial u/\partial r$$

near the outer wall, where ν_x represents the eddy viscosity in the axial direction. Near the inner radial wall,

$$\overline{u'v'} = -\nu_x.\partial u/\partial r.$$

A mixing length expression is used in the inner core region between the two boundary layers, one adjacent to each radial wall. The eddy viscosity ν_x in the high shear region close to either wall is expressed as

$$\nu_x = \left(\frac{r}{R}\right) l_x^2 . \frac{\partial u}{\partial r}$$

where the characteristic length l_x is given as

$$l_x = K\,R\,\ln(R/r)\left[1 - \exp\left\{-R\,\ln\left(\frac{R}{r}\right)\Big/A\right\}\right].$$

The von Karman constant K is 0.405 and A represents the van Driest damping factor defined as $26/Re.\sqrt{\tau_w}$; τ_w is the wall shear stress, expressed as

$$\frac{1}{R_e}.\frac{\partial u}{\partial r}$$

The above expressions for the eddy viscosity and the mixing length apply to the boundary layer adjacent to the outer radius R_o where R_o replaces R. They apply similarly to the boundary layer adjacent to the inner radius R_i under the conditions that

(i) the ratio r/R is reversed becoming R/r, and
(ii) the logarithmic terms are reversed.

A measure of the sublayer thickness is A, the van Driest damping factor. On the basis of available data (Lawn and Elliott, 1971), the value of A for the inner wall was taken to differ from its value of 26 for the outer wall, in the case of small radius ratios, according to $A = 26\,(r^*)^{0.1}$, where r^* represents the radius ratio, R_i/R_o.

A Clauser-type formulation is used for the lower stress region of the inner core, giving

$$\nu_x = 0.0168 U_m \delta^*$$

where δ^* is the displacement area based on the total velocity, i.e.

$$\delta^* = \int_{R_i}^{R_o} r \left(1 - \frac{u}{\overline{U}_m}\right) dr$$

METHOD OF SOLUTION

This is an initial value problem which may be solved by moving in the downstream direction in a single sweep : the initial axial velocity profile is assumed virtually flat at x = o, and computation proceeds at successive spatial increments until the velocities are fully developed.

The axial momentum equation (6) is solved initially, but Δu^{n+1}, the step change in the axial velocity,does not emerge directly on account of the presence of the pressure term P; by applying a integrated form of the continuity equation (3) and separating the pressure term into its axial and radial components, Δp^{n+1} may be evaluated. Knowledge of Δp^{n+1} will then enable Δu^{n+1} to be evaluated from the enlarged tridiagonal system of equations formed from equation (6). Equation (7) is discretised to yield the step change in the radial velocity, Δv^{n+1}.

All terms are evaluated at station n + , except u and v in equation (6), which are projected from upstream locations : this could introduce an error for relatively large axial gradients, but as long as the conditions (see equation (4)) for reducing the original equations apply, the influence of the first order approximation is small.

RESULTS AND DISCUSSION

Developing Velocity Profile

The predicted variation of mean velocity at particular radii along the annular duct is compared with experimental data (Heikal et al., 1977) in Figure 2, in which U_b represents the bulk mean velocity : the experimental data are given with a turbulence promoter.

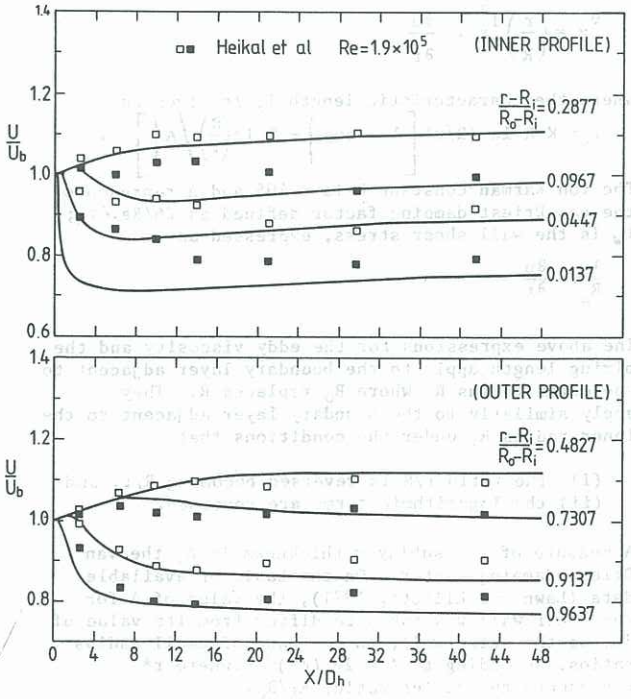

Fig 2. Velocity development in an annulus (r* = 0.25)

Fully Developed Velocity Profile

For non-swirling flow the algorithm is tested against some results (Brighton and Jones, 1964), for fully developed turbulent flow in an annulus for a range of values of the radius ratio r*. By providing artificial roughness on the outer radial surface and placing a screen at the inlet to the test section, fully developed flow was achieved in an entrance length of 34.5 diameters ; by contrast, it was found that fully developed flow in the numerical solution occurred only after 80 hydraulic diameters for a radius ratio of 0.562 and 90 diameters at a radius ratio of 0.375.

Results of the comparison of the numerical model with measurements of mean velocity are shown in Figure 3: the smaller the radius ratio r*, the more skewed is the velocity distribution than the exact solution for laminar flow.

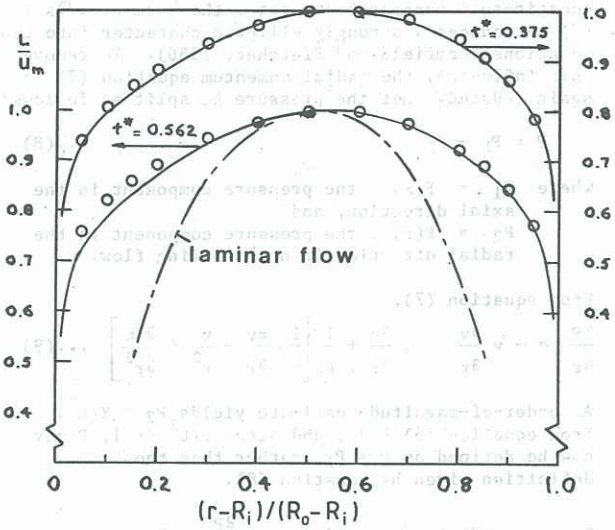

Fig 3. Mean velocity distribution.

The numerical solution approaches the experimental data, at the radius ratio of 0.562, within about 4% ; agreement is better at the radius ratio of 0.375, but not quite as good at the two lowest ratios compared, 0.125 and 0.0625; U_m represents the maximum velocity.

Fully Developed Wall Shear Stresses

The ratio of the fully developed shear stresses at the inner and outer radial walls has been compared with measured data (Kuzay, 1973) taken in a annulus of radius ratio 0.556. Kuzay evaluated shear stress by three methods; the numerical prediction is within 1% of the value obtained by the method which employed a force balance between the wall and the radius of zero shear in the fully developed region. The Preston tube method and the Clauser plot technique yield values which differ from the predicted ratio by 6% and 17.5%, respectively.

Reynolds Stress Profiles

In Figure 4 the Reynolds stress profiles are compared at two streamwise locations (x/D_h = 32, 44.5) with experimental data (Heikal et al., 1977) for a radius ratio of 0.25: τ_2 represents the wall stress at the outer radial boundary. The predicted profiles are within the scatter of the experimental data: in addition, the Reynolds stresses, which approximate more closely to the fully developed profile (x/D_h = 44.5), correlate better with the experimental measurements than those at the other location (x/D_h = 32).

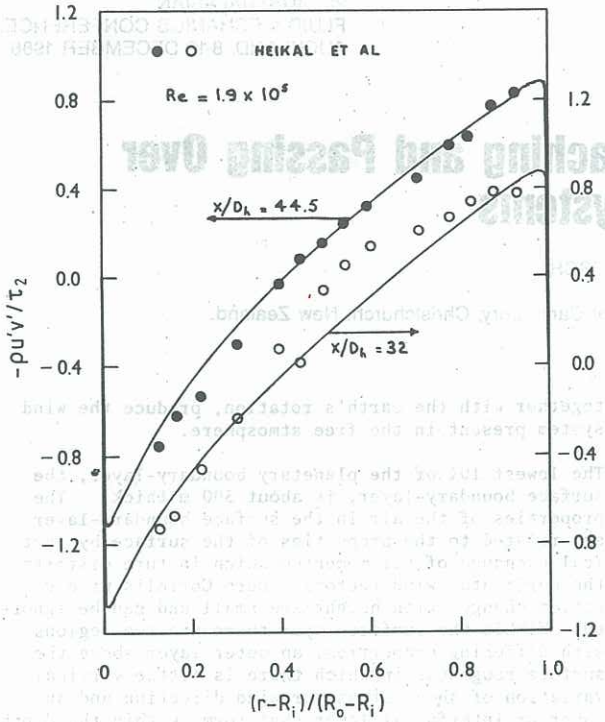

Fig 4. Reynolds stress profile in an annulus ($r^* = 0.25$).

CONCLUSIONS

This investigation has shown that:

(i) The algorithm predicts the developing velocity profile well, within the limits of accuracy of the experimental data : the divergence between the algorithm and the data occurs at low values of x/D_h near the entrance, where the assumptions allowing the governing equations to be reduced are invalid.

(ii) Fully developed velocity profiles are reasonably well predicted.

(iii) The ratio of wall shear stress levels in fully developed flow lies fairly close to the measured quantities.

(iv) The Reynolds stress profiles are closely predicted for developing flow, except near the entrance.

REFERENCES

Armfield, S.W. and Fletcher, C.A.J. (1986): Numerical simulation of swirling flow in diffusers. Int. J. for Numerical Methods in Fluids, to appear.

Bird, R.B., Stewart, W.E. and Lightfoot, E.N. (1960): Transport Phenomena, Wiley, New York.

Brighton J.A. and Jones, J.B. (1964): Fully developed turbulent flow in annuli. J. of Basic Engineering 86, 835-844.

Heikal, M.R.F., Walklate, P.J. and Hatton, A.P. (1977): The effect of free stream turbulence level on the flow and heat transfer in the entrance region of an annulus. Int. J. Heat and Mass Transfer 20, 763-771.

Holland, P.G. and Fletcher, C.A.J. (1985): A single-pass split-group finite element method for convective heat transfer systems. Third Australas. Conf on Heat and Mass Transfer, Melbourne, 389-397.

Kuzay, T.M. (1973): Turbulent heat and momentum transfer studies in an annulus with rotating inner cylinder. Ph.D. thesis, University of Minnesota, Minneapolis, Minnesota, U.S.A.

Lawn, C.J. and Elliott, C.J. (1971): Fully developed turbulent flow through concentric annuli. C.E.G.B. Report RB/B/N 1878.

Schlichting, H. (1955): Boundary Layer Theory, Pergamon, New York.

Yaschin, D., Israeli, M. and Wolfshtein, M. (1984): Numerical solutions of the parabolised three-dimensional steady flow in axially symmetric pipes. Computational Techniques and Applications CTAC-83, North-Holland, Amsterdam, 533-552